

# Modified Microperoxidases Exhibit Different Reactivity Towards Phenolic Substrates

Corrado Dallacosta, Luigi Casella, and Enrico Monzani\*<sup>[a]</sup>

*The reactivity of several microperoxidase derivatives with different distal-site environments has been studied. The distal-site environments of these heme peptides include a positively charged one, an uncharged environment, two bulky and doubly or triply positively charged ones, and one containing aromatic apolar residues. The reactivity in the catalytic oxidation of two representative phenols, carrying opposite charges, by hydrogen peroxide has been investigated. This allows the determination of the binding constants and of the electron-transfer rate from the phenol to the catalyst in the substrate/microperoxidase complex. The electron-transfer rates scarcely depend on the redox and charge properties of the phenol, but depend strongly on the microperoxidase. Information on the disposition of the substrate in the ad-*

*ducts with the microperoxidases has been obtained through determination of the paramagnetic contribution to the <sup>1</sup>H NMR relaxation rates of the protons of the bound substrates. The data show that the electron-transfer rate drops when the substrate binds too far away from the iron and that the phenols bind to microperoxidases at similar distances to those observed with peroxidases. While the reaction rate of microperoxidases with peroxide is significantly smaller than that of the enzymes, the efficiency in the one-electron oxidation of phenolic substrates is almost comparable. Interestingly, the oxyferryl form of the triply positively charged microperoxidases shows a reactivity larger than that exhibited by horseradish peroxidase.*

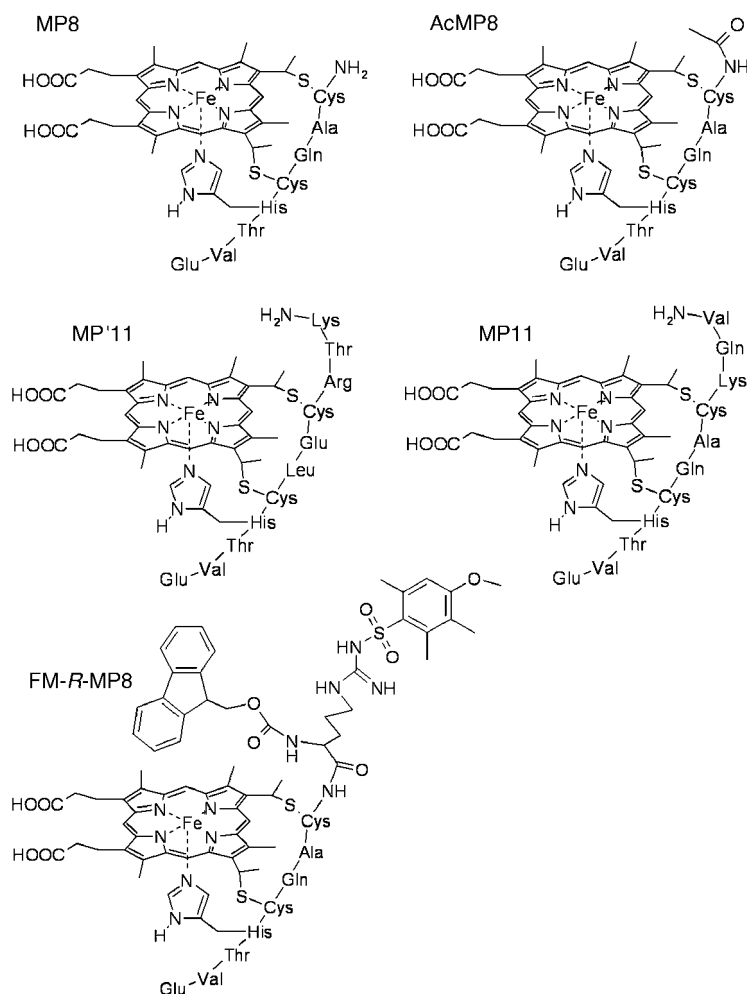
## Introduction

Microperoxidases (MPs) are heme-containing peptides derived from proteolytic digestion of cytochrome c in which the heme is covalently linked to the peptide chain through two thioether bonds.<sup>[1]</sup> The histidine residue, which acts as iron proximal ligand in cytochrome c, is maintained in the MP complexes, while the second axial ligand (Met80 in cytochrome c) is removed by proteolysis, leaving the iron(III) center weakly bound to a water molecule. The best known among MPs is MP8 (Scheme 1), obtained from the peptic and tryptic digestion of horse-heart cytochrome c;<sup>[2–4]</sup> however, by changing the proteolytic conditions or by further chemical modification, several other MP derivatives have been obtained.<sup>[5–10]</sup> MPs are mainly studied as model systems for peroxidases.<sup>[9–20]</sup> Peroxidases catalyze the one-electron oxidation of various substrates in the presence of hydrogen peroxide, through the formation of two active species, namely compound I and compound II, according to Scheme 2. MPs also catalyze the oxidation of various substrates in the presence of H<sub>2</sub>O<sub>2</sub>, although they differ from the enzymes both in terms of structure and reactivity. In particular, MPs contain a heme c, whereas classical peroxidases possess type b heme;<sup>[21]</sup> this may affect the redox properties of the iron centers and will likely influence both the formation rate and the reactivity of the active intermediates involved in the catalytic process. Another difference is that MPs lack the polar residues (Arg and His) that contribute to the typically fast activation process of hydrogen peroxide in the distal site of peroxidases.<sup>[22,23]</sup> The last, but very important, difference is the complete accessibility of the porphyrin ring of MPs by exogenous molecules—in the enzymes usually only the periphery of the heme is accessible to substrates since the cofactor is buried within the protein backbone.<sup>[24,25]</sup> Consequently, the reaction with hydrogen peroxide to produce the active

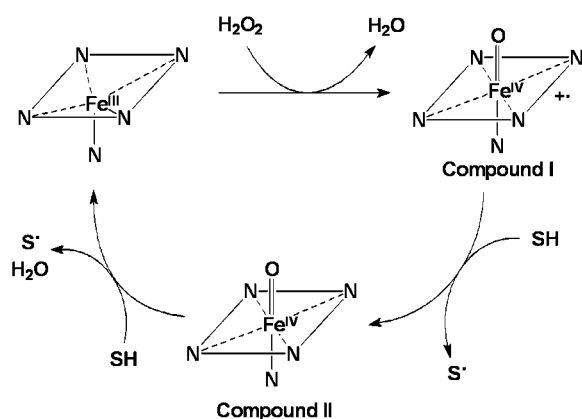
species is much slower in MPs than in peroxidases. The rate constant of this process is around 1000 M<sup>-1</sup> s<sup>-1</sup> with MPs,<sup>[9–12,14]</sup> but reaches values of 10<sup>6</sup>–10<sup>7</sup> M<sup>-1</sup> s<sup>-1</sup> for the enzymes.<sup>[22,23]</sup> In contrast, substrate oxidation is extremely rapid for the MPs compared to the formation of the active species and usually occurs as a fast step in the catalytic cycle. Furthermore, MP-catalyzed reactions are often accompanied by rapid catalyst inactivation.<sup>[9,14,20]</sup>

These problems reduce the possibility for studying the catalytic cycle step that involves the reaction of MPs' active species with reducing substrates and, thus, decrease the importance of MPs as model systems for the reactions of peroxidase active species (compound I or II in Scheme 2) with substrates. In particular, very little is known about the rate of the electron transfer process between reducing substrate and MPs' active species,<sup>[9,14,18]</sup> on the mode of interaction of MPs with the substrate, on their selectivity towards different redox partners, and on the parameters affecting selectivity in catalytic reactions (redox potential, charge, steric hindrance). In the present paper, we compare the behavior of five different MPs, including the known MP8, AcMP8 and MP11, and the new compounds MP'11, obtained from yeast cytochrome c, and FM-R-MP8 (Scheme 1). We have analyzed their catalytic activity in the oxidation of two representative phenolic substrates, tyramine and 3-(4-hydroxyphenyl)propionic acid (HPA), by hydrogen peroxide. In addition, we have studied the interaction of the substrates with MPs by using NMR relaxation experiments.

[a] Dr. C. Dallacosta, Prof. L. Casella, Dr. E. Monzani  
Dipartimento di Chimica Generale, Università di Pavia  
Via Taramelli 12, 27100 Pavia (Italy)  
Fax: (+39) 03825-28544  
E-mail: enrico.monzani@unipv.it



**Scheme 1.** Schematic representation of the microperoxidase derivatives (MPs) employed.



**Scheme 2.** Catalytic cycle of classical peroxidases.

Analysis of all the data leads to the following conclusions: i) polar residues near the heme facilitate the oxidation of the substrate; ii) electrostatic interactions between substrate and MPs control substrate binding but  $\pi$ - $\pi$  stacking interactions

seem to play a very important role; iii) when the phenol binds far away from the heme the electron-transfer rates are considerably reduced; iv) the difference in reactivity between tyramine and HPA is not very dependent on the substrate redox potential.

## Results and Discussion

### Spectral characterization of MP'11

MP'11 contains several groups that undergo a change of protonation state when there is a change in pH. This results in a strong pH dependence of the MP'11 absorption spectrum, which shows, in particular, a change in the iron(III) spin state (from high-spin,  $S=5/2$ , to low-spin,  $S=1/2$ ) upon passing from slightly acidic conditions to neutral or slightly basic pH at micromolar concentration. In order to gain further details on this process, the pH dependence of the Soret band was analyzed from pH 4.5 to 8.0. Figure 1A shows the spectra of the high-spin and low-spin forms whereas Figure 1B shows the absorbance changes versus pH at their maximum absorption. The lack of clear isosbestic points during the spectrophotometric titration and the complex curve for the absorbance changes at 397 nm clearly indicate that more than a single protonation step is involved. A clearer behavior is observed at 407 nm; the fit of the spectral data gave an estimated  $pK_a$  value of  $6.16 \pm 0.03$  for the protonation of the group involved in the change of the iron spin state. Similar behavior was reported for MP11 which showed a spin state change ruled by a protonation step in the same pH range (with reported  $pK_a$  values of 5.8 and 6.3).<sup>[26,27]</sup>

The MP'11 absorption spectrum at pH 7.5 depends on its concentration. Upon dilution of MP'11, from 5 to  $0.06 \mu\text{M}$ , the Soret band maximum shifts from 407 to 402 nm; also, in the visible region the spectrum changes with dilution, from the typical high-spin pattern of the bands, to a mixture of high-spin and low-spin species. Furthermore, after addition of SDS (1% v/v) the spectrum of a relatively concentrated solution of MP'11 (in the micromolar range) at pH 7.5, is typical for high-spin ferric systems, with Soret band at 397 nm. This indicates that the monodispersed MP'11, encapsulated in SDS micelles, is five- or six-coordinated, with a weakly bound water molecule. These observations indicate that the low-spin form of MP'11 at pH 7.5 is not associated with an intramolecular coordination of the iron to the  $\alpha$ - $\text{NH}_2$  or  $\varepsilon$ - $\text{NH}_2$  groups of the Lys residue, or else by the Arg guanidinium group (Scheme 1), but due to an intermolecular coordination, probably by one of the above mentioned groups, from a different MP'11 molecule. Similar behavior was reported for MP11 which, for the intermolecular coordination to iron(III), uses the  $\alpha$ - $\text{NH}_2$  of the Val residue or the  $\varepsilon$ - $\text{NH}_2$  of the Lys residue.<sup>[26,28]</sup> Meanwhile, for the other MP catalysts, the spin properties do not depend on the complex concentration. Moreover, up to  $10 \mu\text{M}$ , the systems show good adherence to the Lambert-Beer law; this indicates

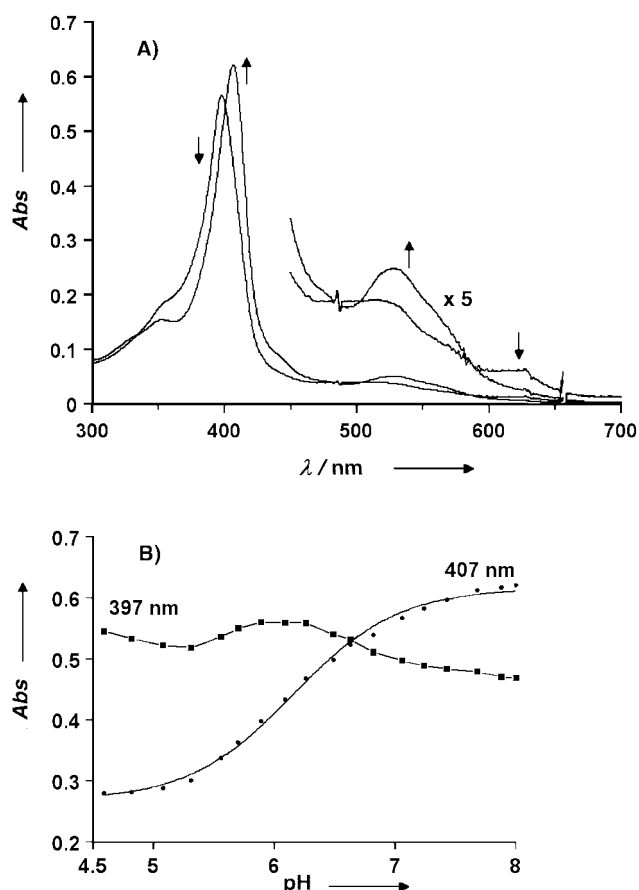
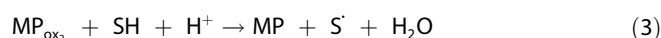
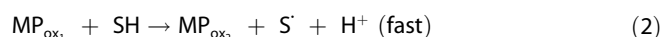


**Figure 1.** A) Electronic absorption spectra of MP 11 (3.5  $\mu\text{M}$ ) at pH 5.9 and pH 8.0 in phosphate buffer (200 mM), at 25°C; 1.0 cm path length. The arrows indicate the direction of the changes upon increasing the pH. B) Absorbance changes with pH at 397 and 407 nm; fitting of the curve at 407 nm has been performed with equation 6.

a prevalent monomeric form within this concentration range (data not shown).

### Kinetics

The catalytic activity of MPs in the oxidations of HPA and tyramine by hydrogen peroxide was studied spectrophotometrically by monitoring the formation of the dimeric products of phenol coupling in the initial phase of the reaction at pH 5.0.<sup>[26]</sup> The catalytic cycle of MPs is thought to be similar to that of peroxidases, like horseradish peroxidase<sup>[20]</sup> (Scheme 2) with first a reaction with  $\text{H}_2\text{O}_2$  followed by two one-electron oxidation steps of substrate molecules.



where  $\text{MP}_{\text{ox}_1}$  and  $\text{MP}_{\text{ox}_2}$  are two active species, one- and two-oxidizing equivalents above the MP iron(III) form, respectively,

the nature of which is not completely clarified.  $\text{S}^\cdot$  is the substrate radical.

In order to analyze the second step of the cycle involving the substrate, the reaction of the MP with hydrogen peroxide must become a faster process than the reduction of the active species by phenol. Thus, the hydrogen peroxide concentration needed during catalysis depends on the second-order rate constant for the reaction of the MP with  $\text{H}_2\text{O}_2$  ( $k_1$ , which has the value of  $680 \pm 10$ ,  $1280 \pm 50$ ,  $76 \pm 2$ ,<sup>[10]</sup> and  $1850 \pm 50 \text{ M}^{-1} \text{ s}^{-1}$  for MP8, MP'11, FM-R-MP8, and MP11, respectively) and on the reactivity towards the substrate. This concentration must be optimized for each catalyst at each substrate concentration in order to have the lowest  $\text{H}_2\text{O}_2$  concentration that warrants the oxidant saturation conditions. Under these conditions, the substrate oxidation reaction is the rate-determining step of the turnover process. Since a significant degradation of MPs occurs during catalysis, the rates were evaluated from the data in the first few tenths of a second. In these conditions, the plots of observed rate versus substrate concentration for MP8,<sup>[20]</sup> AcMP8, and FM-R-MP8 with both tyramine and HPA (Figure 2), and for MP11 with tyramine (Figure 3) show a hyper-

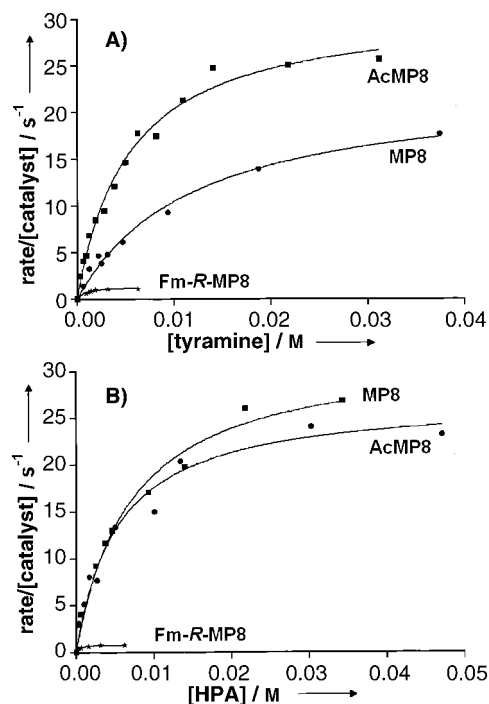


**Figure 2.** Dependence of the substrate oxidation rate by the MP/ $\text{H}_2\text{O}_2$  system on A) tyramine and B) HPA concentration in acetate buffer (0.2 M), pH 5.0, at 25°C.

bolic behavior. Fitting these curves with the Michaelis–Menten equation gives the catalytic parameters  $k_{\text{cat}}$ ,  $K_M$ , and  $k_{\text{cat}}/K_M$  for the two substrates (Table 1). The reaction rates found for each complex and substrate depend linearly on the catalyst concentration (up to 3  $\mu\text{M}$ ) indicating that the eventual aggregation of MPs has negligible effect. Furthermore, the rates as well as the degradation phenomena seem to be independent of the

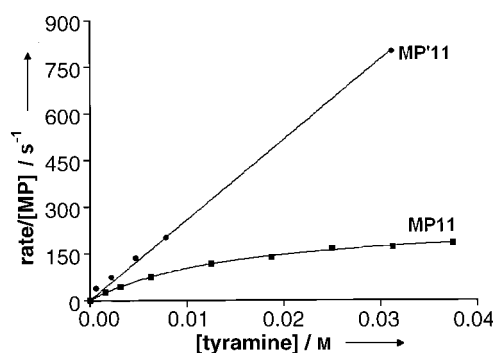


**Figure 3.** Dependence of the tyramine oxidation rate by the MP'11/H<sub>2</sub>O<sub>2</sub> and the MP11/H<sub>2</sub>O<sub>2</sub> systems on substrate concentration in acetate buffer (0.2 M), pH 5.0, at 25°C.

**Table 1.** Kinetic parameters for the catalytic activity of MPs in the oxidation of HPA and tyramine by hydrogen peroxide in acetate buffer (0.2 M), pH 5.0, 25°C.

		$k_{\text{cat}}$ [s <sup>-1</sup> ]	$K_M$ [M]	$k_{\text{cat}}/K_M$ [M <sup>-1</sup> s <sup>-1</sup> ]
MP8	HPA <sup>[a]</sup>	26.9 ± 1.6	0.0053 ± 0.0010	5050 ± 750
MP8	tyramine <sup>[a]</sup>	22.9 ± 1.3	0.0119 ± 0.0015	1920 ± 150
AcMP8	HPA	32 ± 2	0.0071 ± 0.0001	4200 ± 600
AcMP8	tyramine	31 ± 1	0.0053 ± 0.0005	5800 ± 400
FM-R-MP8	HPA	0.80 ± 0.02	0.00034 ± 0.00004	2300 ± 200
FM-R-MP8	tyramine	1.18 ± 0.07	0.0006 ± 0.0001	1900 ± 300
MP'11	HPA	> 800	n.d.	n.d. <sup>[b]</sup>
MP'11	tyramine	> 800	> 0.030	25700 ± 500
MP11	HPA	> 800	n.d.	n.d. <sup>[b]</sup>
MP11	tyramine	257 ± 8	0.015 ± 0.001	16700 ± 700

[a] From ref. [20]. [b] n.d. = not determinable.

nature of the buffer (phosphate or acetate) and ionic strength (data not shown). MP'11 followed a different behavior; in fact, in the experiments performed with tyramine, the oxidation rates increased linearly with substrate concentration up to 30 mM, with no indication of saturation. This implies a high (> 30 mM)  $K_M$  value for tyramine. Thus, only the  $k_{\text{cat}}/K_M$  ratio and an estimate of the lowest value for  $k_{\text{cat}}$  could be obtained (Table 1). It was not possible to reach H<sub>2</sub>O<sub>2</sub> saturation with HPA for both MP'11 and MP11 even at peroxide concentration up to 0.7 M. The rate depended almost linearly on H<sub>2</sub>O<sub>2</sub> concentration in the range studied; this indicates that, in the HPA oxidation by MP'11 and MP11, the peroxide activation, and not the substrate reaction, is the rate-determining step of the catalytic cycle, despite the fact that the  $k_1$  values for these MPs are the largest in the series of MPs studied here. Since this occurs even at low HPA concentration, the  $K_M$  for this substrate should have a small value. In this respect, it should be noted that the substrate concentration cannot be reduced further to prevent excessive catalyst degradation even in the short reaction time monitored. Assuming that MP'11 and MP11 have a similar kinetic approach to the reaction with HPA as the other MPs studied, the following relation must apply:

$$k_1 \times [\text{H}_2\text{O}_2] \ll \frac{k_{\text{cat}} \times [\text{HPA}]}{K_M + [\text{HPA}]} \quad (4)$$

where  $k_1$  is the second-order kinetic constant for the reaction of these MPs with hydrogen peroxide. Thus, the lower limit for the  $k_{\text{cat}}$  value reported in Table 1 depends on the fact that  $k_{\text{cat}}$  should be larger than the highest value of the product  $k_1 \times [\text{H}_2\text{O}_2]$  employed, where  $k_1$  is 1280 ± 50 and 1850 ± 50 M<sup>-1</sup> s<sup>-1</sup> for MP'11<sup>[10]</sup> and MP11, respectively.

### NMR relaxation measurements

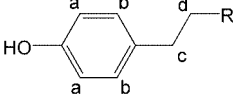
The observed longitudinal relaxation rates ( $1/T_{1,\text{obs}}$ ) for the protons of HPA and tyramine in the presence of variable amounts of MPs are a weighted average between the relaxation rates of the free substrate ( $1/T_{1f}$ ) and the substrate interacting with the MP ( $1/T_{1p}$ ), according to Equation (5):

$$1/T_{1,\text{obs}} = \left[ \frac{1}{T_{1p}} - \frac{1}{T_{1f}} \right] \times \frac{E_0}{K_D + S_0} + \frac{1}{T_{1f}} \quad (5)$$

where  $E_0$  and  $S_0$  are the total (free plus bound) MP and substrate concentrations, respectively, and  $K_D$  is the dissociation constant for the MP-substrate complex.<sup>[29]</sup> As an approximation, the  $K_D$  values for HPA and tyramine were assumed coincident with the  $K_M$  values deduced from kinetic experiments (Table 1). In the case of MP11 and MP'11 the  $K_D$  value of HPA was considered negligible with respect to  $S_0$ , and for MP'11 the  $K_D$  value of tyramine was assumed to be 40 mM. It should be noted, however, that  $K_D$  refers to the dissociation constant of the complex with the MP in the iron(III) form while  $K_M$  refers to the active species of MP. The plots of  $1/T_{1,\text{obs}}$  versus  $E_0/(K_D + S_0)$  for the different protons of HPA and tyramine with the various MPs, show straight lines (data not shown); the  $1/T_{1f}$  and  $1/T_{1p}$  values could be obtained from the y intercept and from the slope of the linear plot

By carrying out relaxation experiments with the low-spin ( $S=1/2$ ) cyanide adducts of the MPs, it was possible to show that the paramagnetic effect of the MPs becomes negligible. Therefore, also the diamagnetic contribution to  $1/T_{1p}$  can be ignored, and  $1/T_{1p} = 1/T_{1M}$ , where  $1/T_{1M}$  is the paramagnetic contribution determined by the interaction of the substrate with the MP complex.<sup>[30]</sup> This contribution originates only from dipolar relaxation and, according to the Solomon–Bloembergen equation, it is possible to correlate  $1/T_{1M}$  to  $1/r^6$ , where  $r$  is the distance between the substrate nucleus and the iron paramagnetic center.<sup>[31,32]</sup> The equation requires knowledge of the correlation time,  $\tau_c$  for the paramagnetic contribution to nuclear relaxation, which depends on the electronic spin correlation time,  $\tau_s$ , on the chemical exchange correlation time,  $\tau_M$ , and on the rotational correlation time,  $\tau_r$  ( $\tau_c^{-1} = \tau_s^{-1} + \tau_M^{-1} + \tau_r^{-1}$ ).  $\tau_M$  is usually longer than the other times and can be neglected, while  $\tau_r$  can be predicted for spherical rigid particles by using the Stokes–Einstein equation:  $\tau_r = \eta \times M / (d \times N_A \times k \times T)$ , where  $\eta$  is the viscosity of the solvent,  $M$  is the molecular weight,  $d$  is the density of the molecule (usually taken to be equal to 10<sup>3</sup> kg m<sup>-3</sup>),  $k$  is the Boltzmann constant, and  $N_A$  is Avogadro's constant.<sup>[33]</sup> Assuming that the catalysts have a rigid spherical

**Table 2.** Iron(III)-proton distances (Å) for HPA and tyramine protons in the complexes between MPs and the phenols in deuterated phosphate buffer (0.2 M), pH 5.0, 25°C. n.d. = not determinable. For tyramine, R = -NH<sub>2</sub>; for HPA, R = -COOH.



MPs	substrate	a [Å]	b [Å]	c [Å]	d [Å]
MP8	HPA	7.4	7.6	7.6	7.6
MP8	tyramine	6.8	7.1	7.2	8.2
AcMP8	HPA	7.6	7.7	7.9	8.0
AcMP8	tyramine	7.4	7.7	7.8	8.6
FM-R-MP8	HPA	9.8	9.6	8.6	9.0
FM-R-MP8	tyramine	n.d.	n.d.	n.d.	n.d.
MP'11	HPA	8.3	8.2	8.4	8.4
MP'11	tyramine	8.8	8.7	9.4	n.d.
MP11	HPA	9.1	8.8	9.5	9.2
MP11	tyramine	8.7	8.6	9.0	n.d.

shape,  $\tau_r$  was calculated to be  $1 \times 10^{-9}$  s. Since  $\tau_s$  is reported to be  $5 \times 10^{-11}$  s for high-spin iron(III) porphyrins,<sup>[34]</sup>  $\tau_r^{-1}$  can be considered negligible with respect to  $\tau_s^{-1}$ . Thus, we assumed that the correlation time for the three MPs is dominated by the electronic relaxation time,  $\tau_c = \tau_s = 5 \times 10^{-11}$  s. The distance,  $r$ , between the substrate protons and the high-spin iron(III) center of the MP complexes were calculated from the  $T_{1M}$  values according to the Solomon-Bloemberger equation; the data are reported in Table 2.

The lack of the contact contribution on the substrate relaxation rates is confirmed by the large iron to proton distances obtained, which are not compatible with direct coordination of the phenol to the iron(III), and by the negligible changes observed in optical spectra of MPs upon addition of up to 50 mM tyramine or HPA at pH 5.0 (data not shown).

To characterize the parameters that rule the substrate discrimination in MPs we studied five MP derivatives containing differences in their distal sites due to the presence of residues with different properties such as charge, polarity and steric hindrance. MP8 has an almost empty and completely accessible distal site which carries the charges of the metal ion and the N-terminal Cys residue, which is protonated at acidic pH (Scheme 1). In AcMP8 the acetylation removes the positive charge of this residue. In MP11 the  $\alpha$ -NH<sub>2</sub> of the terminal Val and the  $\epsilon$ -NH<sub>2</sub> of the Lys residues act as ionizable groups which are relatively free to move over the distal site of the heme, but their position in the peptide skeleton precludes direct coordination to the iron, thus allowing only intermolecular coordination.<sup>[26]</sup> We also prepared the new compound MP'11, from bakers' yeast, which differs from the better known MP11 derived from horse heart due to the different amino acid sequence of the two starting proteins. In particular MP'11 contains the sequence Lys-Thr-Arg in the N-terminal part before the Cys residue that is covalently bound to the heme (Scheme 1).<sup>[35,36]</sup> Therefore, at acidic pH, MP'11 has three positively charged groups which due to the flexibility of their alkyl chain can span the area above the distal site. Presumably, the

$\epsilon$ -NH<sub>2</sub> of the Lys residues, which is N-terminal in MP'11, can approach the iron without significant strain. In spite of this difference, spectroscopic experiments have shown that with MP'11, as for MP11, coordination to the iron by the  $\epsilon$ -NH<sub>2</sub> Lys group can occur only intermolecularly. The new compound FM-R-MP8 (Scheme 1) has been obtained by covalently linking a doubly protected arginine residue to the N-terminal amino group of MP8, by 9-fluorenylmethoxycarbonyl (Fmoc) at  $N_\alpha$  and by a 4-methoxy-2,3,6-trimethylbenzenesulfonyl at  $N_\gamma$ . Thus, in FM-R-MP8, besides the loss of the protonated amino group of MP8, the two aromatic protective groups make the distal site of the complex much more hydrophobic. This is shown by its reduced solubility in pure water, the higher solubility of the complex in water/organic mixtures, and by the larger retention time in the HPLC reverse phase column. The aromatic groups (Fmoc and Mtr) when attached to mobile side chains can sweep a large spatial region, even quite far from the iron center, and certainly introduce steric hindrance in the molecule.

The MPs are thought to catalyze peroxidase-type reactions through a mechanism similar to that of the enzymes, in which the formation of the active species formed by reaction of iron(III) with hydrogen peroxide precedes the reaction with the substrate.<sup>[9-20]</sup> At saturating H<sub>2</sub>O<sub>2</sub> concentration, the hyperbolic dependence of the reaction rates on substrate concentration for MP8,<sup>[20]</sup> AcMP8, and FM-R-MP8 (Figure 2) indicates pre-equilibrium formation of a complex between the substrate and the catalyst active species before the electron-transfer step. As can be seen in Table 1, the efficiency and the selectivity of the catalytic reactions depend on the MP catalyst. The  $k_{cat}$  values measure the rate of electron transfer from the substrate to the MP active species; they depend on the difference in the redox potential of the species involved, on the orbital overlap between the redox partners in the outer-sphere complex, and on the structural rearrangements occurring with the electron transfer, according to Marcus' theory.<sup>[37]</sup> Since the electron-transfer processes are slower than the formation/dissociation of the complex between substrate and catalyst active species (considering that complex formation is driven by hydrophobic and electrostatic interaction, see later, and the  $k_{cat}$  values are not too large, Table 1), the  $K_M$  values can be seen as the reciprocal of the binding constants of the phenols with the MP catalyst oxidant form.

As already found by our group,<sup>[20]</sup> MP8 is more active in the catalytic oxidation of HPA compared to tyramine (Table 1):  $k_{cat}$  is only slightly larger, probably due to the lower redox potential of HPA compared to tyramine (810 and 830 mV vs. Ag/AgCl/KCl saturated, respectively),<sup>[38]</sup> but the  $K_M$  values show a larger difference between the two substrates. The substrate-MP8 interaction is driven by electrostatic interactions as well as by  $\pi$ -stacking interactions between the heme porphyrin ring and the aromatic phenol nucleus. Changing the substrate charge, the electrostatic contribution to the phenol-MP8 binding interaction is reversed. This is confirmed here by the observation that with AcMP8, in which the amino group of MP8 is acetylated, the order of  $K_M$  for the two substrates is reversed and the difference is reduced compared to MP8 (Table 1).

Indeed, for AcMP8 the catalytic constants are very similar for the two substrates.

FM-*R*-MP8 exhibits a peculiar behavior (Figure 2), with  $K_M$  constants ten times smaller than those observed for MP8 and AcMP8, and with very small electron-transfer rates for both substrates. This reactivity can be explained considering the bulky structure of FM-*R*-MP8 around the heme. The substrates probably feel strong  $\pi$ -stacking interactions towards these aromatic groups (very small  $K_M$ ), but their phenolic nuclei are held far from the porphyrin and this reduces the efficiency of electron transfer ( $k_{cat}$ ). As expected, FM-*R*-MP8 shows small selectivity towards the two substrates (similar  $k_{cat}/K_M$  values). MP11 and MP'11 are much more reactive towards tyramine and HPA compared to the other MPs. In the case of tyramine, the high  $K_M$  values observed are consistent with electrostatic repulsion between the substrate and the MPs; the higher positive charge of MP'11 is reflected by the larger  $K_M$  compared to MP11. Interestingly, the  $k_{cat}$  values are remarkably large with these MPs—with MP'11, its value exceeds  $800\text{ s}^{-1}$ . On the other hand, with HPA we were not able to transform substrate oxidation into the rate-determining step of the process even when using high peroxide concentration and low substrate concentration. This indicates that MP11 and MP'11 are highly reactive catalysts towards the substrates, and this is accompanied by high affinity (small  $K_M$ ), probably driven by electrostatic interactions. Also here, only a guess for the lower limit of  $k_{cat}$  is possible (Table 1). The notably high electron-transfer rates observed with MP11 and MP'11 is probably connected to the presence of protonated residues in the distal site of the heme, which increase the reactivity of the active species. A similar effect was observed with HRP; mutating the catalytically important Arg residue with Leu in the enzyme not only reduces compound I-formation rate but strongly decreases the reactivity of the active species with reducing substrates.<sup>[39]</sup>

Another important aspect for rationalization of the reactivity of the MPs towards the substrates is the analysis of their disposition with respect to the heme in the substrate–catalyst complex. The distances of the substrate protons from the iron in these complexes could be estimated by exploiting the effect of the paramagnetic high-spin iron(II) center on the substrate nuclear relaxation. The distance values obtained can be considered a good approximation of what happens when the catalyst is present in its high valent form. The MPs do not have a specific binding site in which the substrate can be hosted and, therefore, we can reasonably expect that the aromatic substrates maintain a high mobility approaching the distal face of the heme. Thus, the pairs of protons labeled a, b, c, and d in the inset in Table 2 give an averaged signal and the calculated distances from the iron(II) center are averaged for all the possible relative dispositions of the bound substrates. The same situation occurs during catalysis since the substrate may approach the MP active species from different positions. In spite of that, it is evident that the phenols have preferential positions while interacting with the MP complexes (Table 2). In MP8 and AcMP8, the aromatic part of tyramine appears to experience a closer approach to the iron with respect to the aliphatic chain, whereas with HPA this is not observed. Surpris-

ingly, the distances to the iron are slightly longer in AcMP8 compared to MP8 even for the positively charged phenol. This may be due to the steric hindrance of the N-terminal modification in AcMP8 or to the loss of the hydrogen bond that may be established by the amino group in MP8 which may assist the binding of the substrate. Interestingly, the distances of HPA protons from iron(II) in the adduct with FM-*R*-MP8 are about 2 Å longer than with MP8 (Table 2). This is consistent with the very small  $K_M$  and  $k_{cat}$  values associated with FM-*R*-MP8 in the turnover experiments. Finally, the high reactivity observed with MP11 and MP'11 is not connected to the binding of the phenol closest to the iron center, since the Fe–proton distances observed here are even longer than with MP8 or AcMP8, probably due to the increased steric hindrance in the heme undecapeptide derivatives. The effect of the positive charges in MP11 and MP'11 peptide chains can be appreciated observing that the electrostatic repulsion felt by the protonated tyramine amino group results in notably larger distance for protons d than for the other protons. Indeed, for protons d, the paramagnetic effect of iron(II) becomes negligible thus preventing an estimate of Fe–proton distance.

In conclusion, this work has shown that the binding of HPA and tyramine to MP complexes occurs with iron–proton distances in the range of 7.4–9.5 Å, which is the same range commonly found for bound phenols in the active site of peroxidases.<sup>[24,25,40]</sup> Both electrostatic and hydrophobic interactions rule the substrate-binding strength and disposition with respect to the heme, and this influences the efficiency of electron transfer from the substrate to the MP active species. Thus, FM-*R*-MP8 has a much reduced activity, which is not only due to low polarity around the heme but also to the fact that the bulky aromatic groups prevent the substrate's approach to the porphyrin. The active species of MP8 and AcMP8 are more reactive than that of FM-*R*-MP8 but still show little activity when compared to the corresponding species formed by classical peroxidases. For instance, by using the same substrates, and at the same pH and temperature, HRP exhibits  $k_{cat}$  values of 3700 and  $230\text{ s}^{-1}$  for HPA and tyramine, respectively.<sup>[41]</sup> The MP active species has an intrinsic reactivity that does not depend only on the substrate interaction mode. In particular, MP11 and MP'11 show that the presence of charged amino acid residues that can approach the iron-oxo group strongly increases  $k_{cat}$ , probably favoring the protonation of the ferryl oxygen required for the transformation of the active species into the iron(II) form. The efficiency of this process is so high in MP11 and MP'11 that their reactivity becomes comparable with that of HRP and, in the case of tyramine oxidation, even larger. To our knowledge this is the highest peroxidase-like activity ever reported for a heme model system.

## Experimental Section

UV/Vis spectra were recorded with Hewlett–Packard HP8452A and HP8453 diode array spectrophotometers. <sup>1</sup>H NMR spectra were recorded at 25 °C on a Bruker AVANCE 400 spectrometer, operating at a proton frequency of 400.13 MHz. HPLC chromatography was performed at room temperature on a Jasco instrument with a MD-

1510 diode array detector by using a SUPELCO C<sub>18</sub> reverse-phase column (10×250 mm); spectrophotometric detection of the HPLC elution profile was performed in the 200–650 nm range. The solvents used for elution were: solvent A, trifluoroacetic acid (TFA) (0.1%) in distilled water, and solvent B, TFA (0.1%) in CH<sub>3</sub>CN; gradient runs were performed with a flow rate of 5 mL min<sup>-1</sup>. The elution was carried out for 6 min with 20% B eluent, followed by a gradient to 55% B in 30 min and then to 100% B in 4 min.

Mass spectra were recorded with a Finnigan LCQ ion trap mass spectrometer; the solution was introduced into the electrospray source at 8 μL min<sup>-1</sup> by using the syringe pump of the instrument; the ESI source operated at 3.5 kV, the capillary temperature was set at 200 °C and its voltage at 10 V; the experiments were performed in positive ion mode. In the MS/MS spectra, the ion of interest was isolated in the ion trap and collisionally activated with 45% ejection amplitude at standard He pressure.

**Sample preparation:** MP8 was prepared from horse-heart cytochrome c (Sigma) according to published procedure,<sup>[20]</sup> and purified by HPLC (retention time: *t<sub>r</sub>* = 17.3 min).

AcMP8 was prepared from MP8 by a slight modification of the literature preparation,<sup>[7]</sup> by placing MP8 (2 mg) in borate buffer (100 mM) pH 9.0, the solution was stirred at room temperature, and 500-fold excess acetic anhydride was added. The solution was then kept at 30 °C for 3 h. The MP derivative was purified by HPLC (*t<sub>r</sub>* = 20.0 min).

MP11 was prepared from horse-heart cytochrome c (Sigma) according to published procedure,<sup>[6]</sup> and purified by HPLC (*t<sub>r</sub>* = 13.6 min).

MP'11 was prepared from yeast (*Saccharomyces cerevisiae*) cytochrome c (Sigma) by a modification of the MP8 preparation. Cytochrome c (50 mg) and pepsin (7 mg) were dissolved in distilled water (10 mL). The pH was slowly adjusted to 2.6, and the solution was incubated overnight at 25 °C in a sealed vessel. Digestion was then interrupted by basification of the solution to pH 8.5. After concentration by ultrafiltration, MP'11 was purified by gel-filtration chromatography, followed by HPLC chromatography (*t<sub>r</sub>* = 15.5 min). The mass spectrum of MP'11 shows the presence of the molecular peak (*m/z* = 1933.7), and analyses of the peaks derived from fragmentation of this ion confirms the peptide sequence. UV/Vis (200 mM phosphate buffer, pH 5.9, high-spin): λ<sub>max</sub> (ε, mol<sup>-1</sup> dm<sup>3</sup> cm<sup>-1</sup>) = 397 (155 000), 498 (9000), 526 sh (8000), 571 sh (4000), 625 (3000); UV/Vis (200 mM phosphate buffer, pH 8.0, low-spin): λ<sub>max</sub> (ε, mol<sup>-1</sup> dm<sup>3</sup> cm<sup>-1</sup>) = 407 (171 000), 529 (13 000), 562 sh (8600). The molar extinction coefficients were determined by the pyridine hemochromogen method.<sup>[42]</sup>

The synthesis of FM-R-MP8 was carried out as follows. Solid MP8 (5 mg) was dissolved in *N,N*-dimethylformamide (500 μL, Carlo Erba, freshly distilled over CaH<sub>2</sub>) and a five fold excess of freshly distilled triethylamine (Sigma) was added. Then, Fmoc-Arg(Mtr)-OPfp (2 mol equiv, Novabiochem) was added and the solution was stirred for 3 h at room temperature. The solvent was dry-evaporated and the solid residue dissolved in the minimum amount of water/CH<sub>3</sub>CN (80/20 (v/v)) mixture and purified by HPLC (*t<sub>r</sub>* = 40.0 min). The mass spectrum of FM-R-MP8 shows the presence of the molecular peak (*m/z* = 2094.2). UV-Vis (CH<sub>3</sub>CN/H<sub>2</sub>O/TFA = 80:20:0.1): λ<sub>max</sub> (ε, mol<sup>-1</sup> dm<sup>3</sup> cm<sup>-1</sup>) = 254 (28 000), 275 sh (15 000), 395 (160 000), 495 (7800), 532 sh (4800), 571 (2800), 620 (3600). The molar extinction coefficients were determined by the pyridine hemochromogen method.<sup>[42]</sup>

**Spectrophotometric acid–base titration of MP'11:** This experiment was performed with solutions of MP'11 (~3.5 μM) at a series

of pH values in the 4.5–8.0 range by using a thermostated, 1 cm path-length cell. Typically, the MP'11 solution, initially in sodium phosphate buffer, pH 4.5 (μ = 0.2 M), at 25.0 ± 0.1 °C, was brought to the given pH by small additions of concentrated sodium hydroxide solution (the dilution was negligible). The pK<sub>a</sub> value for the high-spin to low-spin transition was obtained from the absorbance variations of the Soret band against pH, after correction for dilution. Fitting of the data was done with the equation:

$$Abs = \frac{A + B \times 10^{(pH - pK_a)}}{1 + 10^{(pH - pK_a)}} \quad (6)$$

where *Abs* is the absorbance at each pH value, and *A* and *B* are the absorbancies of the acid and basic forms of MP'11, respectively.

**Dependence of the MP'11 spectrum on the solution concentration:** The spectrum of MP'11 in pH 7.5 phosphate buffer (200 mM), was recorded at different concentrations, from 5–0.06 μM, with 1 or 10 cm path length cuvettes, as appropriate.

**Turnover experiments:** The catalytic oxidations of tyramine and HPA were performed in acetate (50 mM) and phosphate (200 mM) buffer, pH 5.0 at 25 ± 0.1 °C. The reactions were followed spectrophotometrically by monitoring the initial increase with time of the absorbance at 300 nm. These experiments were performed with an Applied Photophysics stopped-flow instrument, model RS-1000, dead time 1 ms, with 1 cm path length, coupled with a HP8452A diode array spectrophotometer. One syringe of the instrument was filled with the MP (3 μM) and variable substrate concentration (HPA: from 0 to 68.0 mM for AcMP8, from 0 to 12.5 mM for FM-R-MP8, and from 0 and 62.5 mM for MP'11 and MP11; tyramine: from 0 to 62.5 mM for AcMP8, from 0 to 12.5 mM for FM-R-MP8, and from 0 to 62.5 mM for MP'11 and MP11; the pH of the solution was always controlled and, where necessary, brought to 5.0). The second syringe was filled with hydrogen peroxide solution in the same buffer. Mixing the two solutions in the cuvette of the instrument reduces the concentration of the reagents to one half. Blank experiments to control the effect of the dilution of MPs in the reaction chamber were performed in the absence of H<sub>2</sub>O<sub>2</sub>; absorbance changes occurred in the mixing time of the instrument, indicating that MPs dilution has negligible effect on the observed reaction rates. At every substrate concentration, H<sub>2</sub>O<sub>2</sub> concentration was optimized by choosing and maximizing the initial rate. The optimized H<sub>2</sub>O<sub>2</sub> concentration was found to increase along with the substrate concentration, passing from 16 to 146 mM for AcMP8, from 13 to 167 mM for FM-R-MP8, and from 13 to 670 mM for MP'11 and MP11, at low and high substrate concentration, respectively. The rates were evaluated from the data in the first few tenths of a second. The transformation of the kinetic data from absorbance s<sup>-1</sup> to m s<sup>-1</sup> was obtained by using the difference in the extinction coefficient between products and reactant at 300 nm (Δε = 1950 m<sup>-1</sup> cm<sup>-1</sup> and 1450 m<sup>-1</sup> cm<sup>-1</sup> for HPA and tyramine, respectively).<sup>[38]</sup> Each experiment was carried out in triplicate.

**Determination of *k*<sub>1</sub> for MP11:** Determination of the catalytic constants for the reaction of MP11 with hydrogen peroxide was performed by studying the dependence of the initial rate of oxidation of *p*-cresol on the oxidant concentration in acetate buffer (200 mM, pH 5.0 at 25 °C) according to a published method.<sup>[9]</sup>

**NMR experiments:** <sup>1</sup>H NMR longitudinal relaxation times (*T*<sub>1</sub>) of HPA and tyramine protons were measured by using the standard inversion recovery method.<sup>[43]</sup> Substrates (15 mM final concentration) were dissolved in 200 mM deuterated phosphate buffer pH 5.0 containing EDTA (0.1 mM) to eliminate interferences by

metal impurities, at  $25 \pm 0.1^\circ\text{C}$ . The  $T_1$  values were then determined at various concentrations of the MPs, ranging from 0 to  $15 \mu\text{M}$  for each substrate and each MP. The time interval between the two impulses in the inversion recovery sequence ranged from 0.05 to 16 s. Each experiment was performed in triplicate. The experiments were also repeated in the presence of NaCN (0.1 mM) in the buffer solution.

**Abbreviations:** HPA: 3-(4-hydroxyphenyl)-propionic acid, tyramine: 4-(2-aminoethyl)-phenol, MP8: microperoxidase-8, AcMP8: *N*-acetyl microperoxidase-8, MP'11: microperoxidase-11 from bakers' yeast, MP11: microperoxidase-11 from horse heart, FM-R-MP8: *N*-Fmoc-Arg(Mtr) microperoxidase-8; ABTS: 2,2'-azinobis(3-ethylbenzo-6-thiazolinesulfonic acid), HRP: horseradish peroxidase, Fmoc-Arg(Mtr)-OPfp: *N*-(9-fluorenylmethoxycarbonyl)-*N*'-4-methoxy-2,3,6-trimethylbenzenesulfonyl-L-arginine pentafluorophenyl ester.

## Acknowledgements

The authors thank the Italian CNR and PRIN of the Italian MIUR for financial support.

**Keywords:** electron transfer • enzyme models • heme proteins • microperoxidases • peroxidases

- [1] A. Lombardi, F. Nistri, V. Pavone, *Chem. Rev.* **2001**, *101*, 3165–3189.
- [2] C. L. Tsou, *Biochem. J.* **1951**, *49*, 362–367.
- [3] J. Aron, D. A. Baldwin, H. M. Marques, J. M. Pratt, P. A. Adams, *J. Inorg. Biochem.* **1986**, *27*, 227–243.
- [4] D. A. Baldwin, H. M. Marques, J. M. Pratt, *J. Inorg. Biochem.* **1986**, *27*, 245–254.
- [5] J. F. Riordan, B. L. Vallee, *Methods Enzymol.* **1967**, *11*, 565–570.
- [6] A. D. Carraway, R. S. Burkhalter, R. Timkovic, J. Peterson, *J. Inorg. Biochem.* **1993**, *52*, 201–207.
- [7] O. Q. Munro, H. M. Marquez, *Inorg. Chem.* **1996**, *35*, 3752–3767.
- [8] R. Ippoliti, A. Picciau, R. Santucci, G. Antonini, M. Brunori, G. Ranghini, *Biochem. J.* **1997**, *328*, 833–840.
- [9] L. Casella, L. De Gioia, G. F. Silvestri, E. Monzani, C. Redaelli, R. Roncone, L. Santagostini, *J. Inorg. Biochem.* **2000**, *79*, 31–33.
- [10] C. Dallacosta, E. Monzani, R. Roncone, L. Casella in *Plant Pperoxidases, Biochemistry and Physiology* (Eds.: M. Acosta, J. N. Rodríguez-López, M. A. Pedreño) Universidad de Murcia, Murcia, **2003**, pp. 97–103.
- [11] D. A. Baldwin, H. M. Marques, J. M. Pratt, *J. Inorg. Biochem.* **1987**, *30*, 203–217.
- [12] P. A. Adams, *J. Chem. Soc. Perkin Trans. 2* **1990**, 1407–1414.
- [13] P. A. Adams, R. D. Goold, *J. Chem. Soc. Chem. Commun.* **1990**, 97–98.
- [14] I. D. Cunningham, J. L. Bachelor, J. M. Pratt, *J. Chem. Soc. Perkin Trans. 2* **1991**, 1839–1843.
- [15] J. S. Wang, H. K. Baek, H. E. van Wart *Biochem. Biophys. Res. Commun.* **1991**, *179*, 1320–1324.
- [16] I. D. Cunningham, G. R. Snare, *J. Chem. Soc. Perkin. Trans. 2* **1992**, 2019–2023.
- [17] I. D. Cunningham, J. L. Bachelor, J. M. Pratt, *J. Chem. Soc. Perkin Trans. 2* **1994**, 1347–1350.
- [18] H. C. Yeh, J. S. Wang, Y. O. Su, W. Y. Lin, *J. Biol. Inorg. Chem.* **2001**, *6*, 770–777.
- [19] J. L. Primus, S. Grunenwald, P. L. Hagedoorn, A. M. Albrecht-Gary, D. Mandon, C. Veeger, *J. Am. Chem. Soc.* **2002**, *124*, 1214–1221.
- [20] C. Dallacosta, E. Monzani, L. Casella, *J. Biol. Inorg. Chem.* **2003**, *8*, 770–776.
- [21] H. B. Dunford, *Heme Peroxidases*, Wiley-VCH, New York **1999**.
- [22] P. J. Ohlsson, T. Yonetani, S. Wold, *Biochim. Biophys. Acta* **1986**, *874*, 160–166.
- [23] H. Anni, T. Yonetani, *Met. Ions Biol. Syst.* **1992**, *28*, 219–241.
- [24] P. R. Ortiz de Mantellano, *Annu. Rev. Pharmacol. Toxicol.* **1992**, *32*, 89–107.
- [25] L. Casella, M. Gullotti, S. Poli, M. Bonfà, R. P. Ferrari, A. Marchesini, *Biochem. J.* **1991**, *279*, 245–250.
- [26] M. T. Wilson, R. J. Ranson, P. Masiakowski, E. Czarnecka, M. Brunori, *Eur. J. Biochem.* **1977**, *77*, 193–199.
- [27] A. M. Jehanli, D. A. Stotter, M. T. Wilson, *Eur. J. Biochem.* **1976**, *71*, 613–616.
- [28] A. D. Carraway, G. T. Miller, L. L. Pearce, J. Peterson, *Inorg. Chem.* **1998**, *37*, 4654–4661.
- [29] L. Banci, I. Bertini, C. Luchinat, *Nuclear and Electron Relaxation: The Magnetic Nucleus-Unpaired Electron Coupling in Solution*, VCH, Weinheim, **1991**.
- [30] C. Redaelli, E. Monzani, L. Santagostini, L. Casella, A. M. Sanangelantoni, R. Pierattelli, L. Banci, *ChemBioChem* **2002**, *3*, 226–233.
- [31] I. Solomon, *Physiol. Rev.* **1955**, *99*, 559–565.
- [32] N. Bloembergen, *J. Chem. Phys.* **1957**, *27*, 572–573.
- [33] I. Bertini, C. Luchinat, *Coord. Chem. Rev.* **1996**, *150*, 77–110.
- [34] G. N. La Mar, F. A. Walker, *J. Am. Chem. Soc.* **1973**, *95*, 6950–6956.
- [35] K. Titani, K. Marita, *J. Biochem.* **1969**, *65*, 247–257.
- [36] F. Sherman, J. W. Steward, J. H. Parker, E. Inhaber, G. J. Slipman, G. J. Puterman, R. L. Gardisky, *J. Biol. Chem.* **1968**, *243*, 5446–5456.
- [37] R. A. Marcus, N. Sutin, *Biochim. Biophys. Acta* **1985**, *811*, 266–273.
- [38] E. Monzani, A. L. Gatti, A. Profumo, L. Casella, M. Gullotti, *Biochemistry* **1997**, *36*, 1918–1926.
- [39] J. N. Rodríguez-López, A. T. Smith, R. N. F. Thorneley, *J. Biol. Chem.* **1996**, *271*, 4023–4030.
- [40] S. Modi, D. V. Behere, S. Mitra, *Biochim. Biophys. Acta* **1989**, *996*, 214–225.
- [41] L. Casella, E. Monzani, M. Gullotti, E. Santelli, S. Poli, T. Beringhelli, *Gazz. Chim. Ital.* **1996**, *126*, 121–125.
- [42] J. H. Fuhrhop, K. M. Smith *Laboratory Methods in Porphyrin and Metalloporphyrin Research*, Elsevier, Amsterdam, **1975**, p. 836.
- [43] R. L. Vold, J. S. Waugh, M. P. Klein, D. E. Phelps, *J. Chem. Phys.* **1968**, *48*, 3831–3832.

Received: May 27, 2004

Early View Article  
Published online on November 8, 2004